3D anisotropic mesh adaptation for functional outputs

Adrien Loseille(*), Alain Dervieux(**) and Frédéric Alauzet(***)

(*)CFD, George Mason University, Fairfax, VA
(**)INRIA - Tropics project Sophia-Antipolis, France
(***)INRIA - Gamma Project Rocquencourt, France
alain.dervieux@inria.fr

ECCM 2010, Paris, may 16-21, 2010

Why can we be interested by mesh adaptation?

Mesh adaptation does:

- **not** simplify you algorithm,
- **not** show an *asymptotical* convergence order higher than non-adaptive algorithms when computing a *smooth* solution.

What we expect is that **mesh adaptation** does:

- improve the *early* phase of convergence,
- produce high order convergence for computing *non-smooth* solutions.

Improving the early phase of convergence

Example: convergence towards a smooth but stiff arctangent solution:

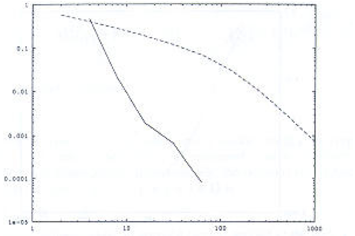

Abscissae: number of nodes, from 0 to 1000; ordinates: L^1 error norm, from 10^{-5} to 1. Upper curve: uniform refinement, Lower curve: adaptive refinement.

Improving the convergence to non-smooth solutions

Example: convergence towards a discontinuous Heaviside-like solution:

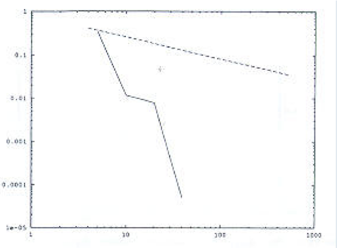

Abscissae: number of nodes, from 0 to 1000; ordinates: L^1 error norm, from 10^{-5} to 1. Upper curve: uniform refinement, Lower curve: adaptive refinement.

Setting mesh adaptation as an optimisation problem:

Starting from the initial ill-posed problem,

Find an optimal mesh $\mathcal{H}_{opt}(u)$ having N vertices such that

$$\mathcal{H}_{opt}(u) = \operatorname{Arg\,min}_{\mathcal{H}} \mathcal{E}(\mathcal{H})$$

- **Which** parameter for optimisation?
- For minimising **what**?

1. Concept of metric-based mesh adaptation
2. Multi-scale mesh adaptation
3. Goal-oriented mesh adaptation

What is a Metric ?

- Canonical Euclidean space:

$$\langle \mathbf{u}\,,\,\mathbf{v}\rangle = {}^t\mathbf{u}\;\mathbf{v} \quad\Longrightarrow\quad \ell(\mathbf{a},\mathbf{b}) = \sqrt{{}^t\mathbf{ab}\;\mathbf{ab}}$$

- Euclidean metric space:
  $\mathcal{M}$: $d \times d$ symmetric definite positive matrix

$$\langle \mathbf{u}\,,\,\mathbf{v}\rangle_{\mathcal{M}} = {}^t\mathbf{u}\mathcal{M}\mathbf{v} \;\Longrightarrow\; \ell_{\mathcal{M}}(\mathbf{a},\mathbf{b}) = \sqrt{{}^t\mathbf{ab}\;\mathcal{M}\;\mathbf{ab}}$$

- Riemannian metric space:
  $(\mathcal{M}(\mathbf{x}))_{\mathbf{x}\in\Omega}$

$$\ell_{\mathcal{M}}(\mathbf{ab}) \;=\; \int_0^1 \sqrt{{}^t\mathbf{ab}\;\mathcal{M}(\mathbf{a}+t\mathbf{ab})\;\mathbf{ab}}\,\mathrm{d}t$$

Definition

- function $\mathbf{M} : \mathbf{x} \in \Omega \mapsto \mathcal{M}(\mathbf{x})$,
- density: $d = \dfrac{1}{h_1 h_2 h_3} = \sqrt{\lambda_1 \lambda_2 \lambda_3}$,
- n anisotropic quotients $r_i = \dfrac{h_i^3}{h_1 h_2 h_3}$
- complexity $\mathcal{C}$:

$$\mathcal{C}(\mathbf{M}) = \int_\Omega d(\mathbf{x})\, d\mathbf{x} = \int_\Omega \sqrt{\det(\mathcal{M}(\mathbf{x}))}\, d\mathbf{x}.$$

Matrix writing

$$\mathcal{M}(\mathbf{x}) = d^{\frac{2}{3}}(\mathbf{x})\, \mathcal{R}(\mathbf{x}) \begin{pmatrix} r_1^{-2/3}(\mathbf{x}) & & \\ & r_2^{-2/3}(\mathbf{x}) & \\ & & r_3^{-2/3}(\mathbf{x}) \end{pmatrix} {}^t\mathcal{R}(\mathbf{x}).$$

Continuous Mesh Framework

The continuous mesh parametrisation to solve mesh adaptation writes:

Discrete	**Continuous**
Element K	Metric tensor $\mathcal{M}$
Mesh $\mathcal{H}$ of Ω_h	Riemannian metric space $\mathbf{M} = (\mathcal{M}(\mathbf{x}))_{\mathbf{x}\in\Omega}$
Number of vertices N_v	Complexity $\mathcal{C}(\mathbf{M}) = \int_\Omega \sqrt{\det(\mathcal{M}(\mathbf{x}))}\, d\mathbf{x}$

- **Main idea:** change the distance evaluation in the mesh generator
  [Vallet, 1992], [Casto-Diaz et Al., 1997], [Hecht et Mohammadi, 1997]

- **Fundamental concept:** **Unit mesh**

Adapting a mesh

$\Updownarrow$ Work in adequate Riemannian metric space

Generating a uniform mesh w.r. to $\mathcal{M}(\mathbf{x})$

$$\mathcal{H} \text{ unit mesh } \iff \forall \mathbf{e},\ \ell_{\mathcal{M}}(\mathbf{e}) \approx 1 \text{ and } \forall K,\ |K|_{\mathcal{M}} \approx \begin{cases} \sqrt{3}/4 & \text{in 2D} \\ \sqrt{2}/12 & \text{in 3D} \end{cases}$$

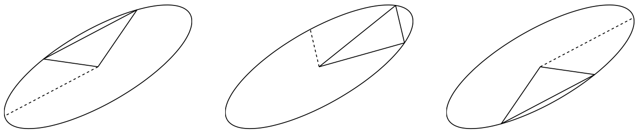

Outline

Minimizing the Interpolation Error in $\mathbf{L}^p$-norm

Starting from the initial ill-posed problem,

> Find an optimal mesh $\mathcal{H}_{opt}(u)$ *having* N vertices such that
> $\mathcal{H}_{opt}(u) = \text{Arg}\min_{\mathcal{H}} \|u - \Pi_{\mathcal{H}} u\|_{\mathbf{L}^p(\Omega)}$

where $\Pi_{\mathcal{H}}$ is the P_1 interpolation on mesh $\mathcal{H}$,

We get a still ill-posed problem:

> Find the continuous mesh $\mathcal{M}_{opt}$ having N vertices such that
> $\mathcal{M}_{opt}(u) = \text{Arg}\min_{\mathcal{M}} \|u - \Pi_{\mathcal{H}} u\|_{\mathbf{L}^p(\Omega)}$

We proposed a continuous mesh framework to solve this problem

Discrete	**Continuous**
Element K	Metric tensor $\mathcal{M}$
Mesh $\mathcal{H}$ of Ω_h	Riemannian metric space $\mathbf{M} = (\mathcal{M}(\mathbf{x}))_{\mathbf{x}\in\Omega}$
Number of vertices N_v	Complexity $\mathcal{C}(\mathbf{M}) = \int_\Omega \sqrt{\det(\mathcal{M}(\mathbf{x}))}\, d\mathbf{x}$
Linear interpolate $\Pi_h u$	**Continuous linear interpolate** $\pi_{\mathcal{M}} u$

$$\mathcal{M}(\mathbf{x}) = d^{\frac{2}{3}}(\mathbf{x})\, \mathcal{R}(\mathbf{x}) \begin{pmatrix} r_1^{-2/3}(\mathbf{x}) & & \\ & r_2^{-2/3}(\mathbf{x}) & \\ & & r_3^{-2/3}(\mathbf{x}) \end{pmatrix} {}^t\mathcal{R}(\mathbf{x}).$$

Continuous Interpolation Error

For any K which is unit for $\mathcal{M}$ and for all u quadratic positive form $(u(\mathbf{x}) = \frac{1}{2}\,{}^t\mathbf{x}\,H\,\mathbf{x})$:

$$\|u - \Pi_h u\|_{\mathbf{L}^1(K)} = \frac{\sqrt{2}}{240}\,\underbrace{\det(\mathcal{M}^{-\frac{1}{2}})}_{\textit{mapping}}\,\underbrace{\mathrm{trace}(\mathcal{M}^{-\frac{1}{2}}\,H\,\mathcal{M}^{-\frac{1}{2}})}_{\textit{anisotropic term}}$$

Continuous interpolation error:

$$\forall \mathbf{x} \in \Omega\,, \quad |u - \pi_{\mathcal{M}} u|(\mathbf{x}) \;=\; \frac{1}{10}\mathrm{trace}\big(\mathcal{M}(\mathbf{x})^{-\frac{1}{2}}\,|H(\mathbf{x})|\,\mathcal{M}(\mathbf{x})^{-\frac{1}{2}}\big)$$

equivalent because:

$$\frac{1}{10}\mathrm{trace}\big(\mathcal{M}(\mathbf{x})^{-\frac{1}{2}}\,|H(\mathbf{x})|\,\mathcal{M}(\mathbf{x})^{-\frac{1}{2}}\big) \;=\; 2\,\frac{\|u - \Pi_h u\|_{\mathbf{L}^1(K)}}{|K|}$$

for any K which is *unit* with respect to $\mathcal{M}(\mathbf{x})$.

Minimizing the Interpolation Error in $\mathbf{L}^p$-norm

A well-posed problem

Find $\mathbf{M}_{opt} = (\mathcal{M}_{opt}(\mathbf{x}))_{\mathbf{x}\in\Omega}$ of complexity N such that

$$
\begin{aligned}
E_{\mathcal{M}_{opt}}(u) &= \min_{\mathcal{M}} \|u - \pi_{\mathcal{M}} u\|_{\mathcal{M},\mathbf{L}^p(\Omega)} \\
&= \min_{\mathcal{M}} \left(\int_\Omega |u(\mathbf{x}) - \pi_{\mathcal{M}} u(\mathbf{x})|^p \, \mathrm{d}\mathbf{x} \right)^{\frac{1}{p}}
\end{aligned}
$$

Solved by a calculus of variations.

Minimizing the Interpolation Error in $\mathbf{L}^p$-norm

Optimal metric

$$\mathcal{M}_{\mathbf{L}^p} \;=\; \underset{❶}{D_{\mathbf{L}^p}} \; \underset{❷}{(\det|H_u|)^{\frac{-1}{2p+3}}} \; \underset{❸}{\mathcal{R}_u^{-1}} \; \underset{❹}{|\Lambda|} \; \mathcal{R}_u$$

❶ Global normalization: to reach the constraint complexity N

$$D_{\mathbf{L}^p} = N^{\frac{2}{3}} \left(\int_\Omega (\det|H_u|)^{\frac{p}{2p+3}} \right)^{-\frac{2}{3}} \quad \text{and} \quad D_{\mathbf{L}^\infty} = N^{\frac{2}{3}} \left(\int_\Omega (\det|H_u|)^{\frac{1}{2}} \right)^{-\frac{2}{3}}$$

❷ Local normalization: sensitivity to small solution variations, depends on $\mathbf{L}^p$ norm chosen

❸ Optimal anisotropy directions based on Hessian eigenvectors

❹ Diagonal matrix of anisotropy strengths, defined from the absolute values of Hessian eigenvalues

Multi-Scales Mesh Adaptation

In contrast to error equidistribution (L^∞-based), the L^p allows capturing the different scales. Example on a non-regular solution:

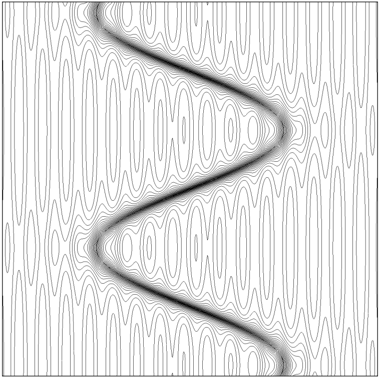

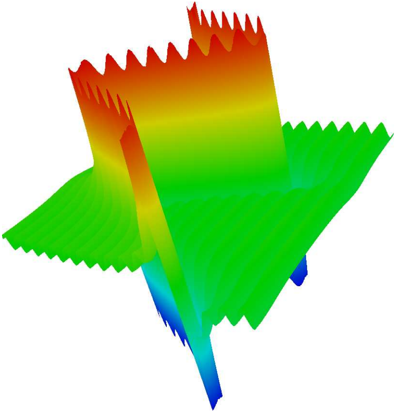

Example on a non-regular solution (cont'd):

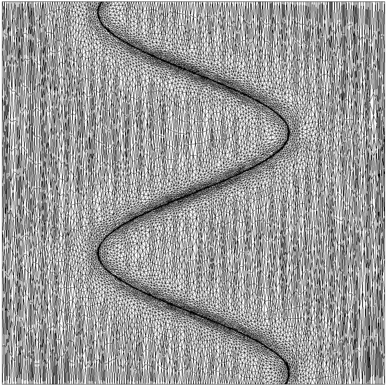

L^2-adaptation

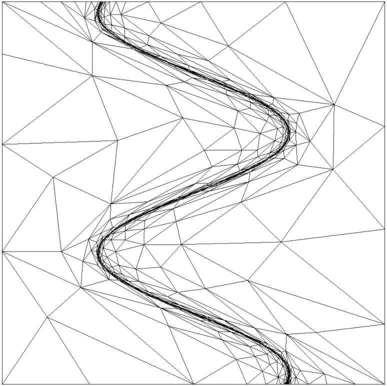

L^∞-adaptation

Mesh Adaptation Algorithm for PDEs

Mesh adaptation is a non-linear problem

$\Longrightarrow$ an iterative process is required to converge the couple mesh-solution

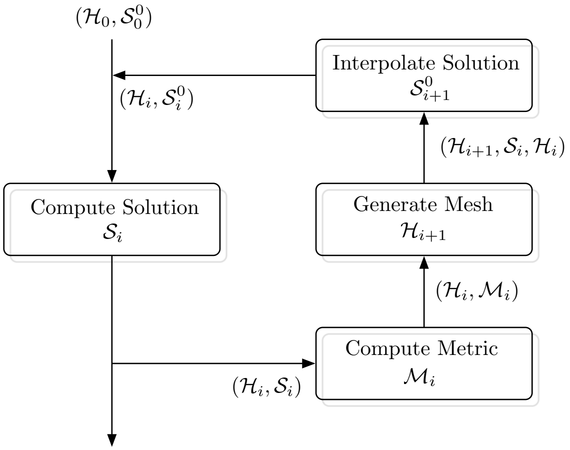

A Supersonic Aircraft

Supersonic CFD simulation on the supersonic business jet provided by Dassault Aviation

Objective: modelling the sonic boom

- 1.6 Mach
- an angle of attack of 3 degrees
- an altitude of $45,000$ feet

Simulation carried out in serial on a MacPro

- 2.66 GHz Intel Xeon processor
- 4 GB of memory
- approximately 48 hours of CPU for the whole process (22 millions of tetrahedra)

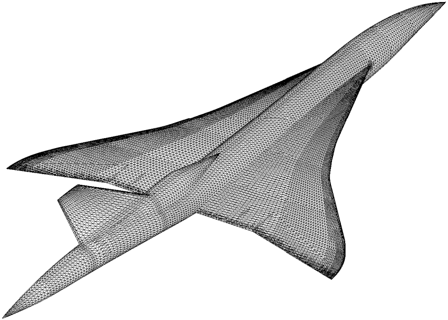

Aircraft geometry

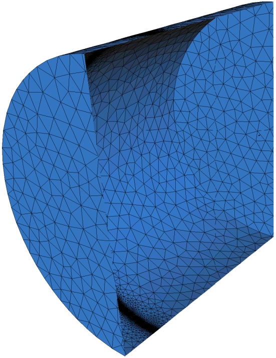

Computational domain

Aircraft size = 36m, mesh size from 2mm to 30cm

Domain size (meters):
$x : [-225,\ 2025] \quad y : [-1200,\ 1200] \quad z : [-1200,\ 1200]$

- Adapted mesh with $\mathbf{L}^2$ norm on the Mach Number
  - $\approx$ 4.2 million vertices
  - $\approx$ 25.1 million tetrahedra

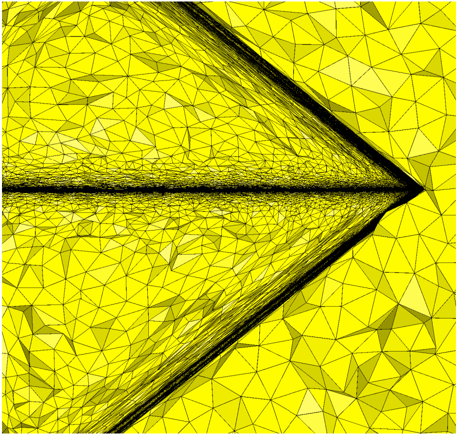

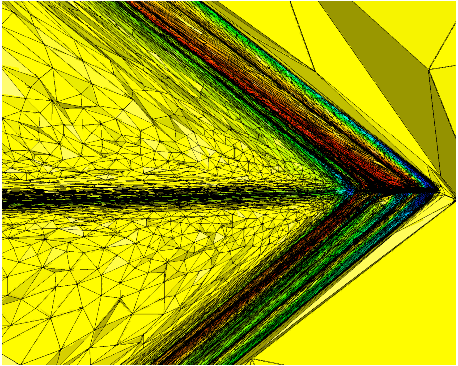

Mesh refinements propagate 2km

A Supersonic Aircraft

- Adapted mesh with $\mathbf{L}^2$ norm on the Mach Number
  - $\approx$ 4.2 million vertices
  - $\approx$ 25.1 million tetrahedra

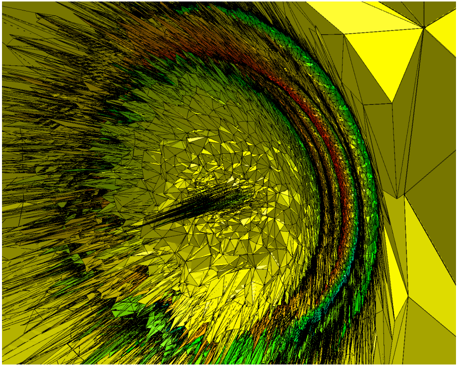

Mesh behind the aircraft

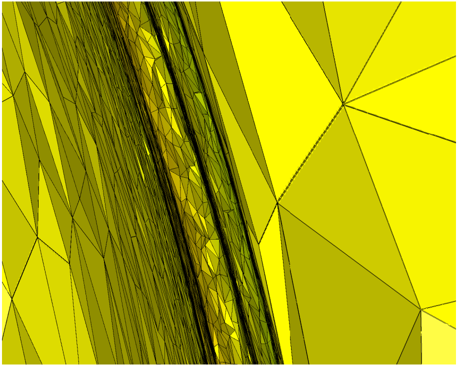

After 2km of propagation
mesh size is $\approx$ one meter

A Supersonic Aircraft

- Mach Number iso-values
  - Solution accurately propagated in the whole domain
  - All shocks are accurately captured

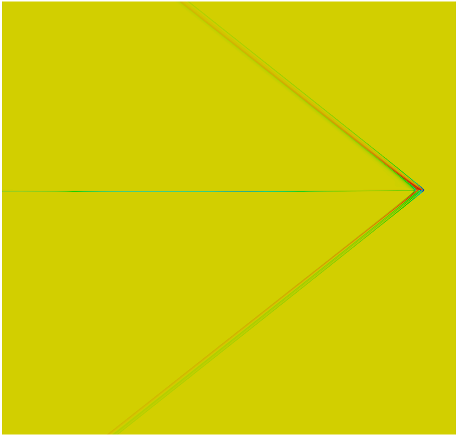

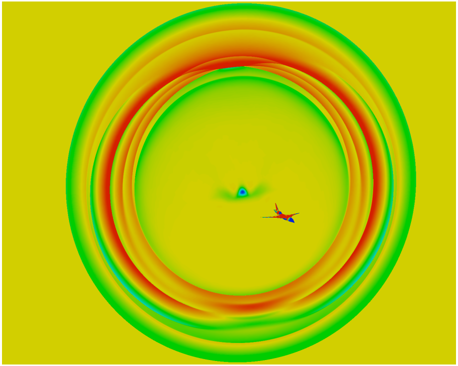

A Supersonic Aircraft

- Mach Number iso-surfaces
  - Mach cone clearly appears
  - Solution accurately propagated in the whole domain

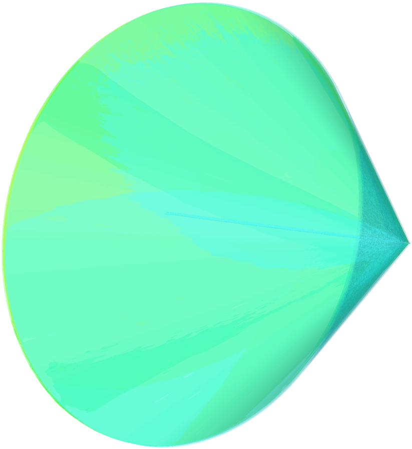

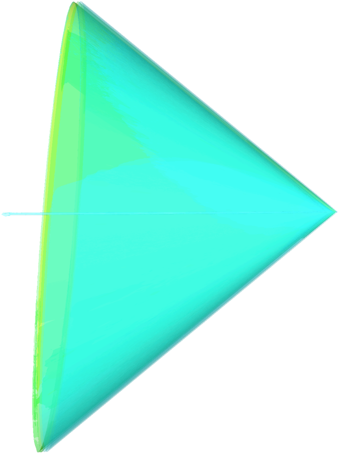

Anisotropic ratio

$$\text{ratio} = \sqrt{\frac{\min_i \lambda_i}{\max_i \lambda_i}} = \frac{\max_i h_i}{\min_i h_i},$$

Anisotropic ratio		
$1 < \text{ratio} \leq 2$	29 609	0.12 %
$2 < \text{ratio} \leq 3$	123 788	0.49 %
$3 < \text{ratio} \leq 4$	190 705	0.76 %
$4 < \text{ratio} \leq 5$	227 993	0.91 %
$5 < \text{ratio} \leq 10$	1 032 940	4.12 %
$10 < \text{ratio} \leq 50$	3 795 329	15.13 %
$50 < \text{ratio} \leq 100$	3 205 727	12.78 %
$100 < \text{ratio} \leq 1\,000$	15 446 359	61.60 %
$1\,000 < \text{ratio} \leq 10\,000$	102 4491	4.09 %
Mean ratio	288	

Anisotropic quotient

$$\text{quo} = \frac{\max_i h_i^3}{h_1 h_2 h_3},$$

Anisotropic quotient		
$1 < \text{quo} \leq 2$	7 423	0.03 %
$2 < \text{quo} \leq 3$	36 325	0.14 %
$3 < \text{quo} \leq 4$	57 309	0.23 %
$4 < \text{quo} \leq 5$	71 293	0.28 %
$5 < \text{quo} \leq 10$	376 558	1.50 %
$10 < \text{quo} \leq 50$	1 268 085	5.06 %
$50 < \text{quo} \leq 100$	692 184	2.76 %
$100 < \text{quo} \leq 1000$	3 667 454	14.62 %
$10^3 < \text{quo} \leq 10^4$	7 709 552	30.74 %
$10^4 < \text{quo} \leq 10^5$	9 359 580	37.32 %
$10^5 < \text{quo}$	1 831 199	7.30 %
Mean quo	30877	

Mesh convergence for various aircraft geometries

Measured from L^2 norm of Mach deviation with respect to a very fine 10M nodes mesh, shown for meshes of 1M to 4M nodes.

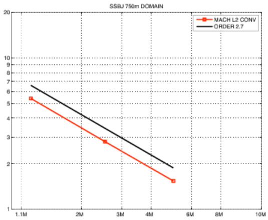

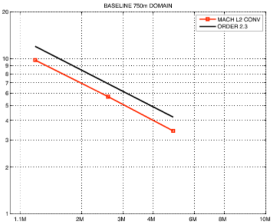

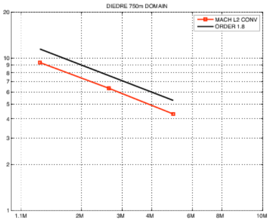

Outline

Motivations for Goal-Oriented Mesh Adaptation

Outputs of interest

- area of interest is generally known

$\Longrightarrow$ Computation of a functional $j(\mathbf{w})$ that depends on physical solution $\mathbf{w} = (\rho, \mathbf{u}, p)$.

- Performance of solution $\mathbf{w}$ evaluated thanks to $j(\mathbf{w})$

Exemples

- vorticity in wake $j(\mathbf{w}) = \displaystyle\int_\gamma \|\nabla \wedge (\mathbf{u} - \mathbf{u}_\infty)\|_2^2 \, \mathrm{d}\gamma$
- sonic boom $j(\mathbf{w}) = \displaystyle\int_\gamma \left(\frac{p - p_\infty}{p_\infty}\right)^2 \mathrm{d}\gamma$
- drag, lift: use to quantify the performance of a design , etc...

Goal: Take into account this supplementary information in the adaptive process

Geometrical adaptation (*Hessian-based*)

[Castro Diaz et Al., 1997], [Habashi et Al., 2000], [Frey et Alauzet, 2005], ...

- Genericity, does not depend on the EDP and on the numerical scheme
- Anisotropy easily deduced

Goal-oriented mesh adaptation (*Adjoint-based*)

[Venditti et Darmofal, 2002], ...

- Explicit use of the EDP
- Strong dependency on the numerical scheme
- Anisotropy hard to prescribe

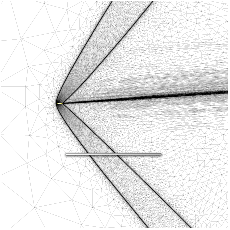

- Given a functional $j(w)$
- We only know w_h
- How to control $j(w) - j(w_h)$

Formal Resolution

Continuous and discrete equations

$$(\Psi(w), \phi) = 0 \quad \text{and} \quad (\Psi_h(w_h), \phi_h) = 0$$

Continuous and discrete adjoint equations

$$(\frac{\partial \Psi}{\partial w}(w)\phi, p) = (g, \phi) \quad \text{and} \quad (\frac{\partial \Psi_h}{\partial w}(w_h)\phi_h, p_h) = (g, \phi_h)$$

Adjoint estimation

- Dual formula [Giles et Süli, 2002]

$$j(w) - j(w_h) \approx (g, w - w_h) \quad = \quad \underbrace{-(p, \Psi(w_h))}_{\textit{A posteriori}} \quad = \quad \underbrace{(p_h, \Psi_h(w))}_{\textit{A priori}}$$

A priori error estimation [D, L and A, 2008]

$$
\begin{aligned}
j(w) - j(w_h) \quad &= \quad \underbrace{(g, w - w_h)}_{\textit{Approximation error}} = \underbrace{(g, w - \Pi_h w)}_{\textit{Interpolation error}} + \underbrace{(g, \Pi_h w - w_h)}_{\textit{Implicit error}} \\
(D.A.E.) \quad &= \quad (g, w - \Pi_h w) + \left(\frac{\partial \Psi_h}{\partial w}(\Pi_h w)(\Pi_h w - w_h), p_h \right) \\
(T.D.) \quad &= \quad (g, w - \Pi_h w) + (\Psi_h(\Pi_h w), p_h) - (\Psi_h(w_h), p_h) + R_1 \\
&= \quad (g, w - \Pi_h w) + (\Psi_h(\Pi_h w), p_h) - (\Psi_h(w), p_h) \\
&+ \quad ((\Psi_h - \Psi), p_h) + R_1 \\
(T.D.) \quad &= \quad (g, w - \Pi_h w) + \left(\frac{\partial \Psi_h}{\partial w}(w)(\Pi_h w - w), p_h \right) \\
&+ \quad ((\Psi_h - \Psi)(w), p_h) + R_2
\end{aligned}
$$

Formal Resolution

A priori error estimation [D, L and A, 2008]

$$
\begin{aligned}
j(w) - j(w_h) &= \underbrace{(g, w - w_h)}_{\textit{Approximation error}} = \underbrace{(g, w - \Pi_h w)}_{\textit{Interpolation error}} + \underbrace{(g, \Pi_h w - w_h)}_{\textit{Implicit error}} \\
(Only\ \ C.\ Terms) &= (g, w - \Pi_h w) + \left(\frac{\partial \Psi}{\partial w}(w)(\Pi_h w - w), p \right) \\
&+ ((\Psi_h - \Psi)(w), p) + R_3 \\
(C.A.E.) &= ((\Psi_h - \Psi)(w), p) + R_3
\end{aligned}
$$

Use of anisotropic mesh adaptation to reach asymptotic convergence even in singular cases

$$p_h \longrightarrow p$$

$$\Psi(W) = \nabla.\mathcal{F}(W) = 0$$

From the previous analysis it results

$$\begin{aligned} j(w) - j(w_h) &\approx \int_\Omega P \;\left(\nabla.\mathcal{F}_h(W) - \nabla.\mathcal{F}(W)\right) \mathrm{d}\Omega + \mathrm{BT} \\ &= \int_\Omega \nabla.P \;\left(\mathcal{F}(W) - \mathcal{F}_h(W)\right) \mathrm{d}\Omega + \mathrm{BT} \\ &= \int_\Omega \nabla.P \;\left(\mathcal{F}(W) - \Pi_h\mathcal{F}(W)\right) \mathrm{d}\Omega + \mathrm{BT} \end{aligned}$$

Properties

- interpolation error on the Euler fluxes
- weighted $\mathbf{L}^1$ interpolation error
- sum of interpolation errors

Solve this problem in the continuous framework

Find $\mathbf{M}_{opt} = (\mathcal{M}_{opt}(\mathbf{x}))_{\mathbf{x}\in\Omega}$ of complexity N such that

$$E(\mathcal{M}_{opt}) = \min_{\mathcal{M}} \int_\Omega \nabla.P\left(\mathcal{F}(W) - \pi_{\mathcal{M}}\mathcal{F}(W)\right) \mathrm{d}\Omega + \mathrm{BT}$$

A calculus of variations gives

$$\mathcal{M}_{opt} = \mathcal{M}_{opt}^{\mathbf{L}^1}\left(\sum_{i=1}^{5}(\sum_{j=1}^{3}|\nabla_{x_j}P_h(W_i)|\,|H(\mathcal{F}_{x_j}(W_i))|)\right)$$

Application to sonic boom :

- Adjoint functional :

$$j(W) = \int_\gamma \left(\frac{p - p_\infty}{p_\infty} \right)^2 \mathrm{d}\gamma$$

- Adaptation variable : Mach number

Comparisons between adjoint and hessian

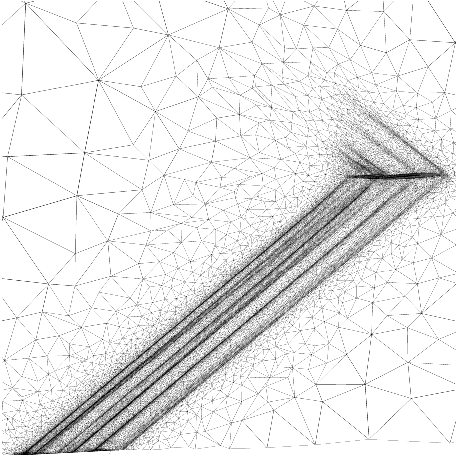

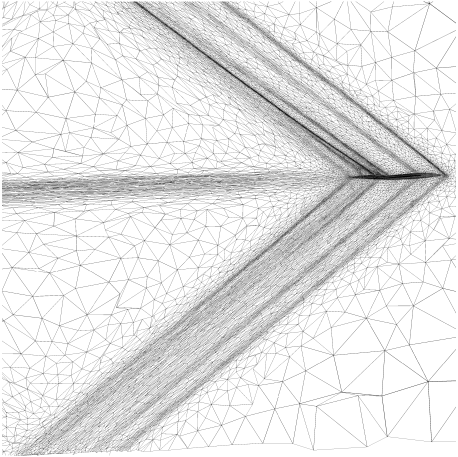

Comparisons between adjoint and hessian

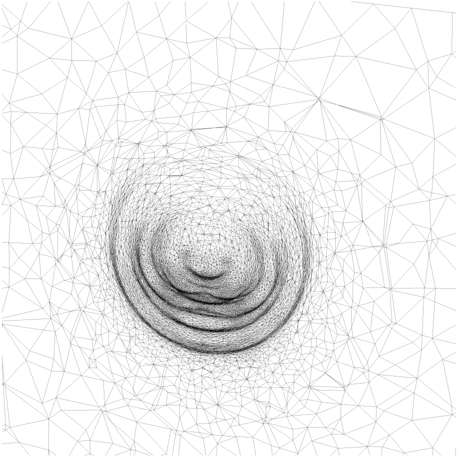

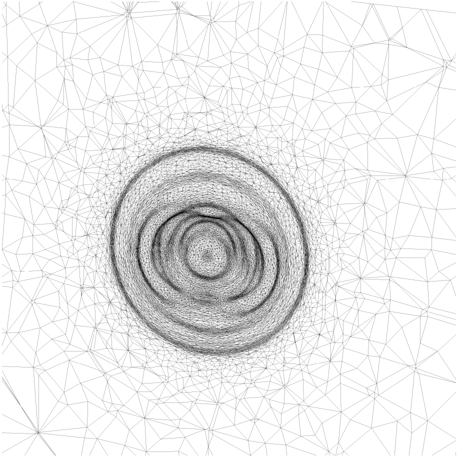

Comparisons between adjoint and hessian

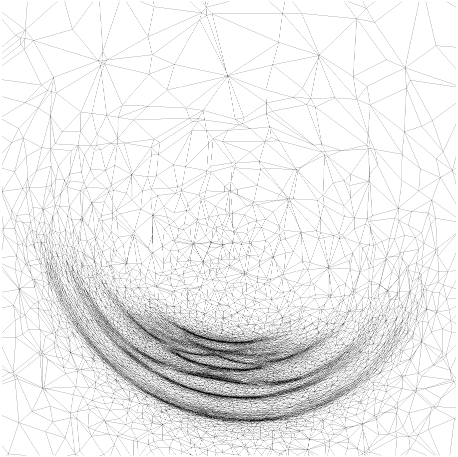

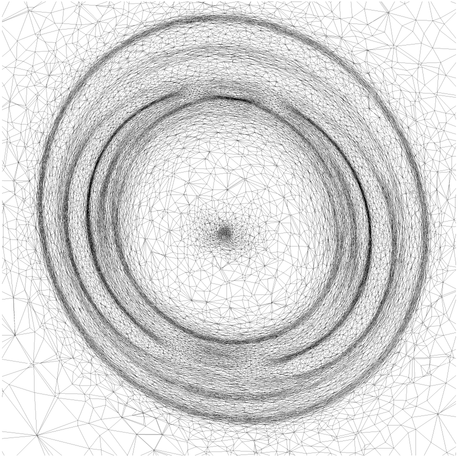

Comparisons between adjoint and hessian

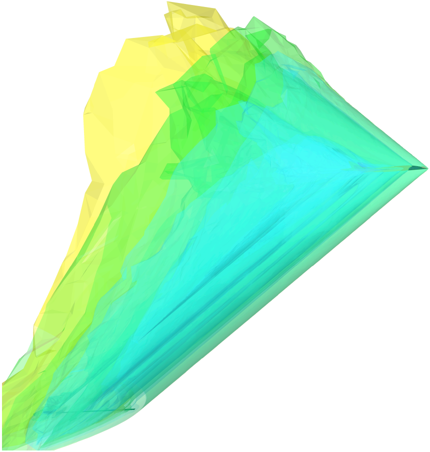

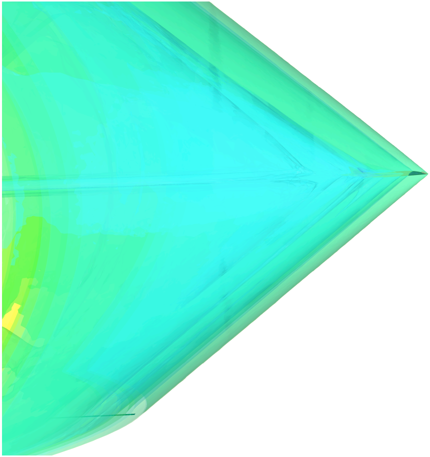

Comparisons between adjoint and hessian

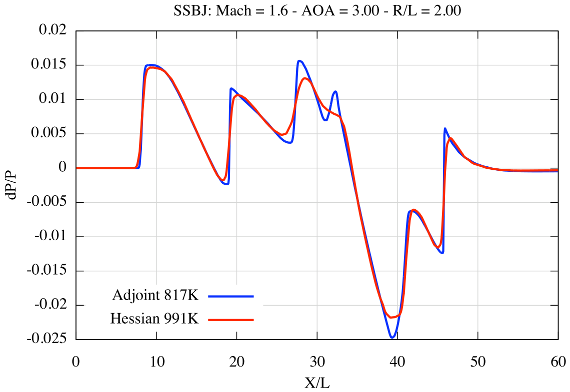

Anisotropic ratio

$$\text{ratio} = \sqrt{\frac{\min_i \lambda_i}{\max_i \lambda_i}} = \frac{\max_i h_i}{\min_i h_i},$$

Anisotropic ratio	Adjoint-based		Hessian-based	
$1 < \text{ratio} \leq 2$	87 152	1.81 %	63 900	1.34 %
$2 < \text{ratio} \leq 3$	344 171	7.15 %	254 689	5.33 %
$3 < \text{ratio} \leq 4$	408 150	8.48 %	326 727	6.84 %
$4 < \text{ratio} \leq 5$	383 587	7.97 %	333 693	6.99 %
$5 < \text{ratio} \leq 10$	1 417 279	29.43 %	1 464 200	30.67 %
$10 < \text{ratio} \leq 50$	2 160 709	44.87 %	2 318 963	48.57 %
$50 < \text{ratio} \leq 100$	14 589	0.30 %	11 748	0.25 %
Mean ratio	11.404		11.721	

$$\text{quo} = \frac{\max_i h_i^3}{h_1 h_2 h_3},$$

Anisotropic quotient	Adjoint-based		Hessian-based	
$1 < \text{quo} \leq 2$	20 670	0.43 %	15 391	0.32 %
$2 < \text{quo} \leq 3$	98 030	2.04 %	71 910	1.51 %
$3 < \text{quo} \leq 4$	135 076	2.80 %	99 694	2.09 %
$4 < \text{quo} \leq 5$	140 389	2.92 %	105 367	2.21 %
$5 < \text{quo} \leq 10$	570 124	11.84 %	459 995	9.64 %
$10 < \text{quo} \leq 50$	1 635 197	33.96 %	1 635 882	34.27 %
$50 < \text{quo} \leq 100$	731 548	15.19 %	855 954	17.93 %
$100 < \text{quo} \leq 1000$	1 435 724	29.81 %	1 502 571	31.47 %
$10^3 < \text{quo} \leq 10^4$	48 955	1.02 %		
$10^4 < \text{quo} \leq 10^5$	4	0.00 %		
$10^5 < \text{quo}$	1	0.00 %		
Mean quo	109.74		117.24	

Computation of wing tip vortices :

- Adjoint functional :

$$j(W) = \int_\gamma \|\nabla \wedge (\mathbf{u} - \mathbf{u}_\infty)\|_2^2 \, d\gamma$$

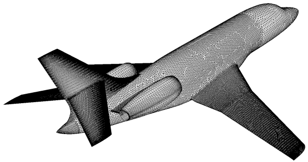

- Adaptation variable : Mach number

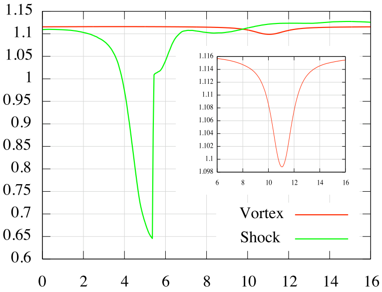

Vorticity 100m behind the Falcon:

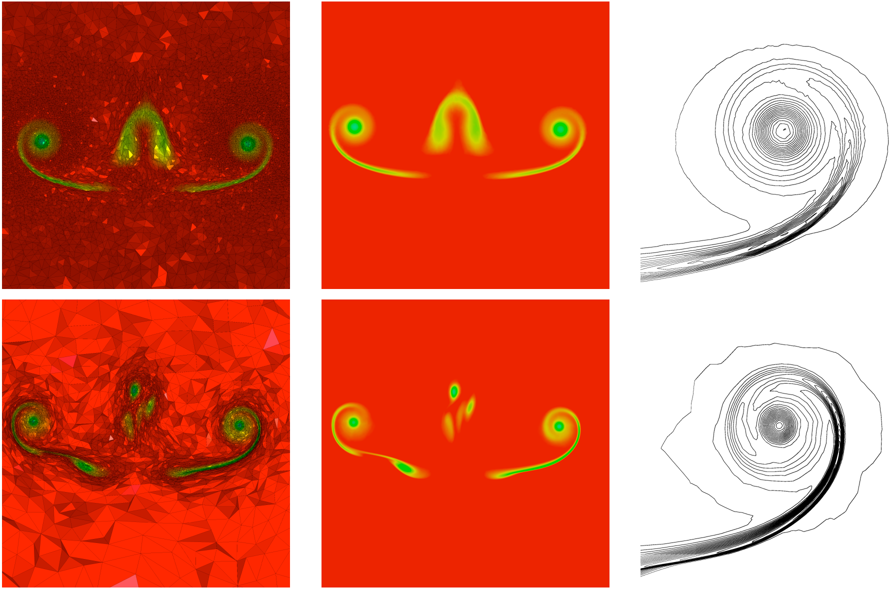

Vorticity 200m behind the Falcon:

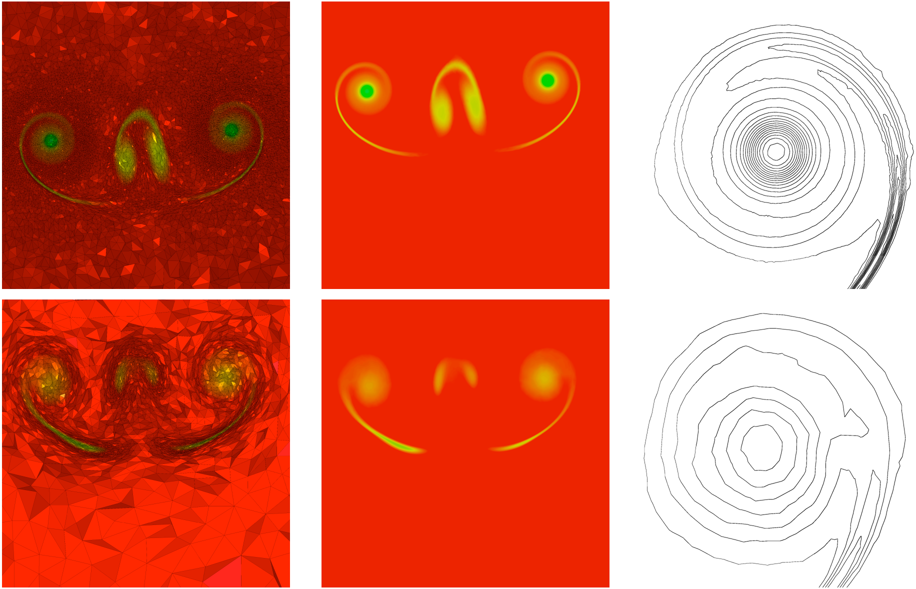

Vorticity 400m behind the Falcon:

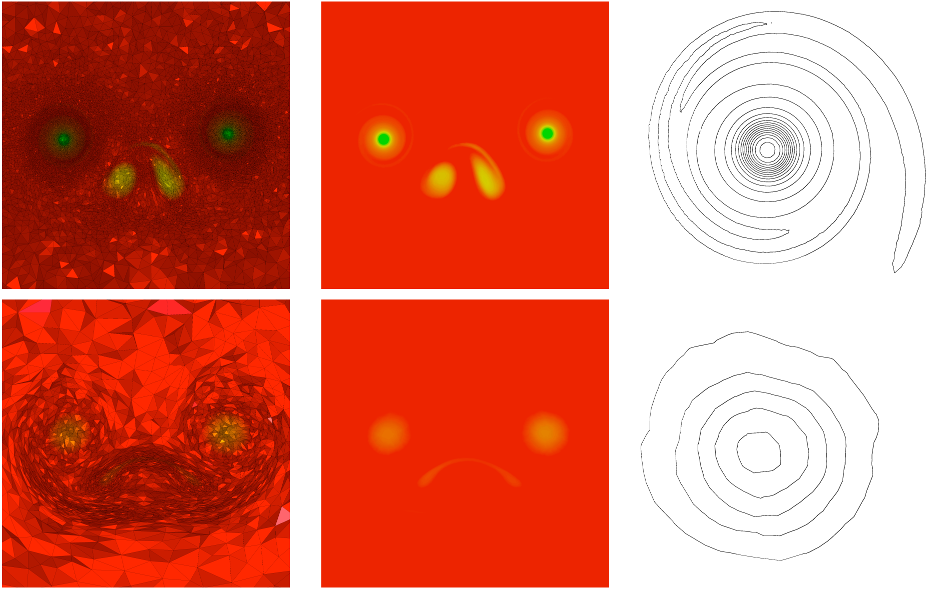

Adapted meshes :

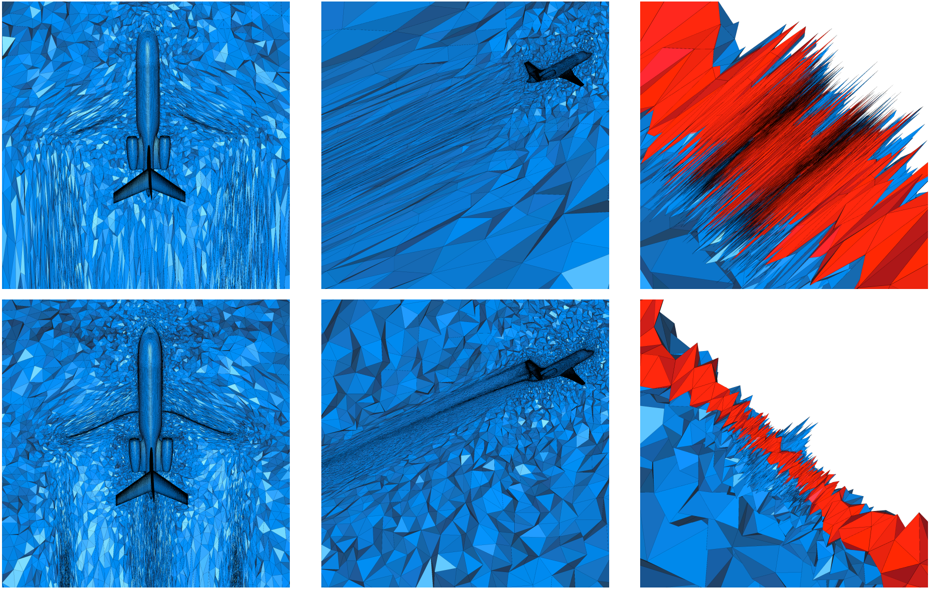

Vorticity iso-surfaces :

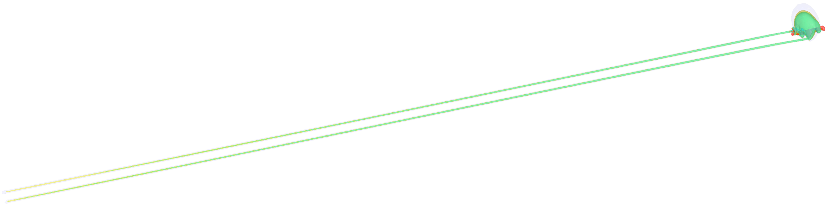

Concluding remarks (1)

Two adaptive techniques have been presented:

- The multi-scale anisotropic mesh adaptation.
- The goal-oriented anisotropic mesh adaptation.

- The multi-scales method shows high-order mesh convergence, although not many theoretical arguments pleade for this.
- The goal-oriented method (which shows also high-order mesh convergence for the functional, not discussed here) far supersedes the multi-scale method for well specified goals.

Concluding remarks (2)

- Extension to unsteady simulations are currently addressed. See bibliography of the abstract and the other presentations by Alauzet and Olivier.
- Extension to other PDE models can be considered, with no a priori limitation to CFD.

Thank you for your attention

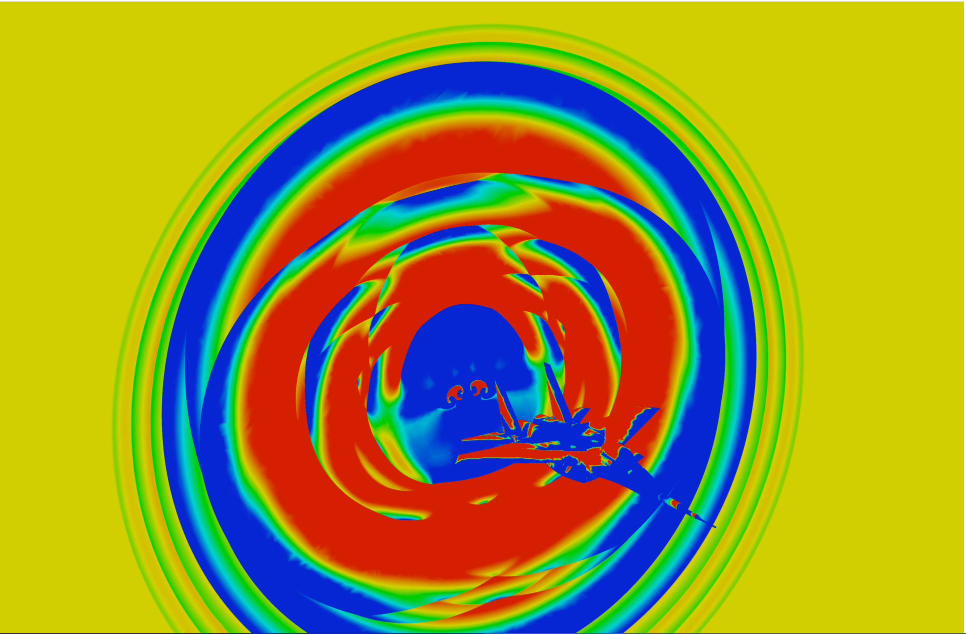

Business supersonic flight

- Financial motivation
- Environmental constraints

Physical phenomenon

- Multi-scale: from millimeter to kilometer
- Shock waves

State of the art: no actual low boom design

- Projects: Dassault Aviation (HISAC), Aerion Corp., GulfStream Aerospace, NASA, JAXA
- Innovative concept: Quiet Spike
- Full scale experiments very expensive and difficult

Quiet spike concept

- Initial geometry: F15
- Quiet Spike [Henne et Al., 2004, US Patent], Gulfstrean Aerospace
- Flight condition test, NASA Dryden Flight Research Center, 2006

NASA Dryden Flight Research Center Photo Collection
http://www.dfrc.nasa.gov/Gallery/Photo/index.html
NASA Photo: ED06-0184-13 Date: September 27, 2006 Photo By: Carla Thomas

NASA F-15B #836 in flight with Quiet Spike attached.

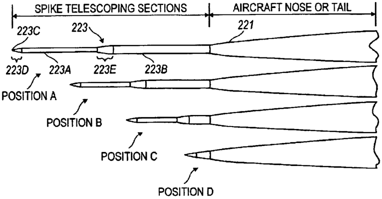

F15-Spike

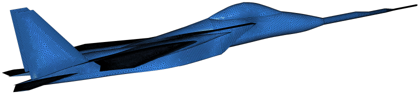

Gulfstream Nasa strategy [Howe et Al., 2008], [Henne et Al., 2008], [Waithe, 2008]

1. Near-field: $R/L < 0.3$ unstructured adaptation
   - Mandatory to capture the complexity of the flow
2. Mid-field: $R/L \geq 0.3$ structured solver [Laflin et Al., 2006]
   - Mandatory to avoid solution diffusion

90 *feet (27m) below the aircraft, the [adapted] unstructured has dissipated significantly, . . . , unstructured solver alone seems impractical*

F15-Spike: pressure field obtained at a distance of 67m (220ft) below the aircraft

F15-Spike

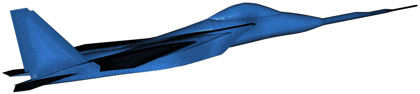

Gamma strategy

1. Near-field/mid-field: coupling multi-scale and goal-oriented unstructured mesh adaptation
   - Pressure field observed on the spike: $j(w) = \int_\gamma \left(\frac{p-p_\infty}{p_\infty}\right)^2$
   - Multi-scale adaptation on the local Mach number

F15-Spike: Accurate pressure field obtained at 120m below the aircraft with a mesh of 3.8M of ver. within 5 days of computation on 4 processors and 15G of RAM

$\Longrightarrow$ anisotropic mesh adaptation reduces solver dissipation

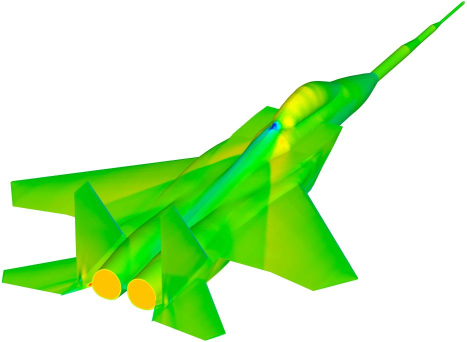

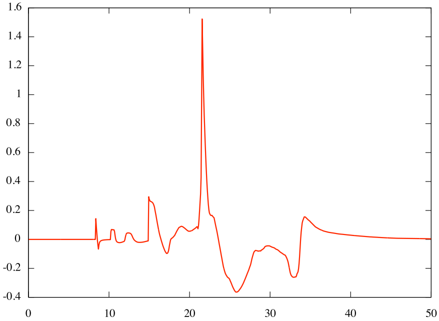

1.6
1.4
1.2
1
0.8
0.6
0.4
0.2
0
-0.2
-0.4
0
10
20
30
40
50

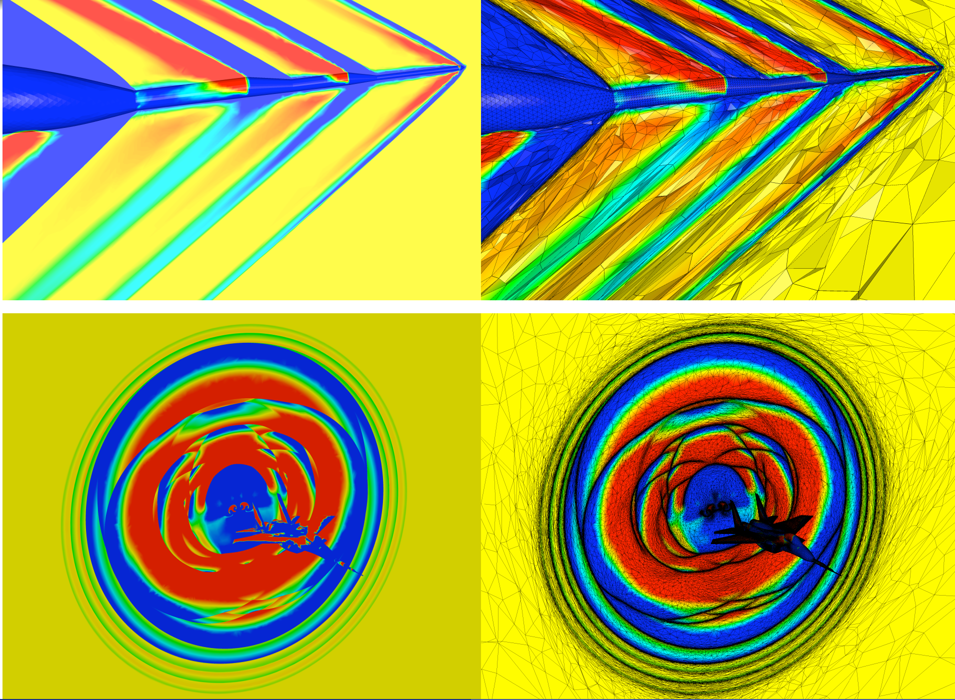

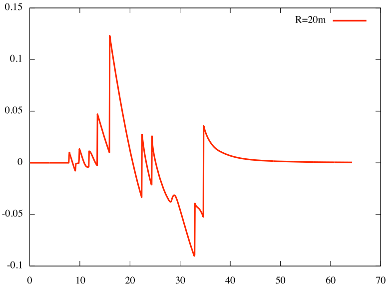
R=20m
0.15
0.1
0.05
0
-0.05
-0.1
0
10
20
30
40
50
60
70

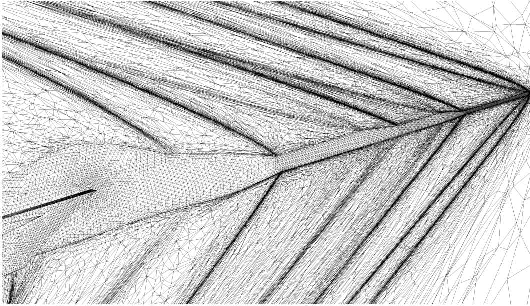

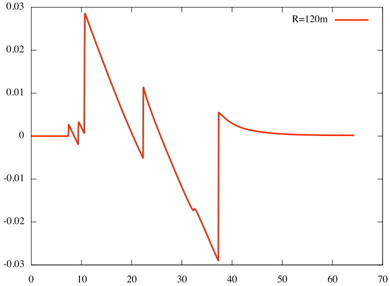
R=120m
0.03
0.02
0.01
0
-0.01
-0.02
-0.03
0
10
20
30
40
50
60
70